# Supporting Information for *Nanoscale*

## Fluorine-Free Preparation of Titanium Carbide MXene Quantum Dots with High Near-infrared Photothermal Performances for Cancer Therapy

*Xinghua Yu[a], Xingke Cai[a], Haodong Cui[b], Seung-Wuk Lee[a], Xue-Feng Yu[b]*, and Bilu Liu[a]**

[a] Tsinghua-Berkeley Shenzhen Institute, Tsinghua University, Shenzhen 518055, P.R. China.

[b] Institute of Biomedicine and Biotechnology, Shenzhen Institutes of Advanced Technology, Chinese Academy of Sciences, Shenzhen 518055, P. R. China

Corresponding authors. xf.yu@siat.ac.cn (XFY), bilu.liu@sz.tsinghua.edu.cn (BL)

**S1. Materials.** The bulk $Ti_3AlC_2$ powders were purchased from a commercial supplier (Forsman, China). 3-(4,5-dimethyl-2-thiazolyl)-2,5-diphenyl-2-H-tetrazolium bromide (MTT) was bought from Sigma-Aldrich. PBS (pH=7.4), fetal bovine serum (FBS), DMEM, trypsin-EDTA, and penicillin-streptomycin were purchased from Gibco Life Technologies (AG, Switzerland). PEG-$NH_2$ was purchased from Shanghai Ponsure Biotech, Inc., China. All other chemicals used in this work were analytical reagent grade and used without further purification.

**S2. Preparation of MXene QDs.** The MXene QDs were prepared using a fluorine-free method developed in this research. Specifically, the preparation of MXene QDs was based on a facile liquid exfoliation technique involving ultrasound probe sonication followed by bath sonication of powders of bulk $Ti_3AlC_2$. In brief, $Ti_3AlC_2$ powders (25 mg), TBAOH (10mL), and water (25 mL) were added into a sealed conical tube (with a volume of 50 mL). The mixture was sonicated with a sonic tip for 6 h at a power of 480 W. The ultrasonic frequency was from 19 to 25 kHz and the ultrasound probe worked in a 2s ON and 4s OFF fashion. The dispersions were further bath sonicated continuously for another 10 h at a power of 300 W. The resulting dispersion was centrifuged for 20 min at 7,000 rpm, and the supernatant containing MXene QDs was collected gently. Later, the MXene QDs were precipitated out from the supernatant solution by centrifuging for 30 min at 12,000 rpm. The precipitate, which contains MXene QDs was repeated water rinsing and re-suspended in PBS or ultrapure water for further use. In our work, the MXene QDs were dispersed in water based media. Specifically, for NIR optical absorption characterization, the solvent is water. For the cell and animal experiments, the solvent is PBS, which is a standard media for biological experiments.

**S3. Modifications of MXene QDs with PEG.** To coat PEG on MXene QDs, the MXene QDs (1 mg) dispersed in $H_2O$ (5 mL) was mixed with of PEG-$NH_2$ (5 mg). After ultra-sonication for 20 min and stirring for 4 h, excess PEG molecules were removed by centrifugation at 12,000 rpm and repeated water rinsing. The final PEG-modified MXene QDs were re-suspended in PBS or ultrapure water for further use.

**S4. Characterization.** SEM images and EDS mapping of the as-received bulk $Ti_3AlC_2$ powders were taken on a field emission SEM (FESEM, 5.0 kV, HITACHI SU8010, Japan). TEM images, STEM images and EDS mapping of MXene nanosheets and QDs were taken on the Tecnai $G^2$ F30 S-Twin TEM at an electron acceleration voltage of 300 kV. AFM studies were performed on the drop-casted MXene samples on $Si/SiO_2$ substrates (Bruker Dimension® Icon$^{TM}$). X-ray photoelectron spectroscopy (XPS) measurements were conducted on the Thermo Fisher ESCALAB 250Xi XPS. UV–vis–NIR absorption spectra were recorded on an Infinite M200 Pro TECAN GENIOS with QS-grade quartz cuvettes at room temperature. The concentrations of MXene QDs were determined by ICP-AES (7000DV, PerkinElmer).

**S5. Photothermal evaluation of MXene QDs.** To assess the photothermal effect of the as-synthesized MXene QDs, various concentrations of MXene QD solutions were irradiated under an 808 nm laser at a power density of 1.0 W/cm$^2$ for 300s. An IR thermal imaging camera (FLUKE Ti25) was used to record temperatures of the solution at different times. To evaluate the NIR stability of MXene QDs, MXene QDs (50 ppm) were irradiated for 10 min at a power density of 1.0 W/cm$^2$ and then the laser was turned off. This procedure was repeated for five times to assess the photostability of MXene QDs.

**S6. Calculations of photothermal conversion efficiency.** Following Roper et al.'s report,[1] the total energy balance of the system can be considered as

$$\sum_i m_i C_{pi} \frac{dT}{dt} = Q_{QD} + Q_{Dis} - Q_{surr} \quad (1)$$

where $m$ and $C_p$ are the mass and heat capacity of water, $T$ is the temperature of water, $Q_{QD}$ is the energy inputted by MXene QDs, $Q_{Dis}$ is the energy entrance by the sample cell, and $Q_{Surr}$ is heat conduction away from the system. $Q_{QD}$, represents heat dissipated on the MXene QDs surface under the irradiation of 808 nm laser:

$$Q_{QD} = I(1 - 10^{-A_{808}})\eta \quad (2)$$

Where $I$ is laser power incidentally (in unit of mW), $A_{808}$ is the absorbance of the MXene QDs at a wavelength of 808 nm, and $\eta$ is the photothermal conversion efficiency from incident light energy from laser to thermal energy. In addition, $Q_{Dis}$ is heat dissipated from light absorbed by the sample cell itself, and it can be measured independently by a sample cell containing pure water without MXene QDs. $Q_{QD}$ is linear relationship with temperature for the outgoing thermal energy, as the following equation:

$$Q_{Surr} = hS(T - T_{Surr}) \quad (3)$$

where $h$ is heat transfer coefficient, $S$ is the surface area of the sample cell, and $T_{Surr}$ is the temperature of the surroundings.

Once the power of the laser is defined, the heat input ($Q_{QD}$ + $Q_{Surr}$) will be finite. Since the heat output $Q_{QD}$ is increased along with the temperature increasing according to the equation (3), the system temperature will increase to a maximum when the heat input is equal to heat output:

$$Q_{Dis} = Q_{Surr-Max} = hS(T_{Max} - T_{Surr}) \quad (4)$$

where $Q_{Surr\text{-}Max}$ is the heat conduction away from the system by air when the temperature of sample cell reaches equilibrium, and $T_{MAX}$ is the equilibrium temperature. The 808 nm laser

photothermal conversion efficiency ($\eta$) can be determined by substituting equation (2) for $Q_{QD}$ into equation (4) and rearranging to get

$$\eta = \frac{hS(T_{Max}-T_{Surr})-Q_{Dis}}{I(1-10^{-A_{808}})} \quad (5)$$

where $Q_{Dis}$ was measured independently, the $T_{Max}$-$T_{Surr}$ was 20 ℃according to Fig. S4a, $A_{808}$ is the absorbance of MXene QDs at 808 nm. Thus, only the *hS* remains unknown for calculating $\eta$. In order to get the *hS*, a dimensionless driving force temperature, $\theta$ has a relation with the maximum system temperature, $T_{Max}$

$$\theta = \frac{T-T_{Surr}}{(T_{Max}-T_{Surr})} \quad (6)$$

and a sample system time constant $\tau_s$

$$\tau_s = \frac{\sum_i m_i C_{P,i}}{hS} \quad (7)$$

which is substituted into equation (1) and rearranged to yield

$$\frac{d\theta}{dt} = \frac{1}{\tau_s}\left[\frac{Q_{QD}+Q_{Dis}}{hS(T_{Max}-T_{Surr})} - \theta\right] \quad (8)$$

At the cooling period of MXene QDs aqueous dispersion, the light source was shut off,

The $Q_{QD}$ + $Q_{Dis}$ =0, reducing the following equation

$$dt = -\tau_s \frac{d\theta}{\theta} \quad (9)$$

and integrating, giving the expression

$$t = -\tau_s, ln\theta \quad (10)$$

Therefore, time constant for heat transfer from the system can be determined by applying the linear time data coming from the cooling stage versus negative natural logarithm of driving force temperature (Fig. S4b). In addition, the *m* is 1 g and the *C* is 4.2 J/g. Thus, according to equation (7), the *hS* is deduced to be 18.3 mW/°*C*. Substituting this value of *hS* into equation (5), the 808 nm laser photothermal conversion efficiency ($\eta$) of MXene QDs can be calculated to be 52.2%.

**S7. Cell culture.** HeLa, MCF-7, U251, and HEK 293 cells were cultured in DMEM medium. All the cell culture media were supplemented with 10% fetal bovine serum (FBS) and 1% streptomycin/penicillin. Cells were kept at 37 ℃ in a humidified atmosphere with 5% $CO_2$.

**S8. *In vitro* toxicity and safety studies.** HeLa cells were seeded at a density of 5,000 cells/well in 96-well plates and incubated overnight. Then, the cells were incubated with MXene QDs solution at different concentrations (6.25, 12.5, 25, 50, and 100 ppm) for 48 h. After that, the excess MXene QDs were removed by washing twice with PBS. A standard MTT assay was used to analyze the cell viabilities. Similar experiments were carried out on MCF-7, U251, and HEK 293 cells to further evaluate the safety of MXene QDs on different types of cells.

**S9. PA Imaging.** To evaluate the linearity of the PA signals as a function of the concentrations of MXene QDs, different concentrations of MXene QDs dissolved in purified water were used for *in vitro* PA signal detection. As for *in vivo* PA imaging, experimental mice were administrated with MXene QDs solution (1 mg/mL, 50 μL) via *i.t.* injection. PA imaging was carried out both prior to and after each injection.

**S10. *In vitro* PTT.** The HeLa cells were treated with MXene QDs with the concentrations of 25 and 50 ppm for 12 h before laser irradiation. Different laser power densities were used to irradiate the cells. After irradiation, a standard MTT assay was used to calculate the relative cell viabilities.

**S11. *In vivo* PTT.** Female Balb/c mice (5 weeks old) were purchased from Guangdong Medical Laboratory Animal Center Co. Ltd. The Administrative Committee on Animal Research in Tsinghua University approved the protocols for all animal assays in this study.

The tumor model was generated by subcutaneously injecting 100 μL of PBS containing 1× $10^6$ HeLa cells into the back of each mouse. The tumor volume was calculated according to the formula: tumor volume ($mm^3$) = 1/2 × length × $width^2$.

When the tumor volume reached about 100 $mm^3$, the mice were divided into three groups (n = 5 in each group) including group 1: PBS, group 2: MXene QDs, and group 3: MXene QDs followed with irradiation by an 808 nm NIR laser at a power of 0.5 W/$cm^2$. For group 1, the mice were received an *i.t.* injection of 20 μL of PBS. For group 2 and group 3, the mice were received an *i.t.* injection of 20 μL of MXene QDs (0.5 mg/kg), respectively. For the PTT treatments group 3, after injection, the mice were irradiated by the 808 nm laser at a power density of 0.5 W/$cm^2$ for 5 min. During the irradiation, the local temperature of tumor was monitored using thermal infrared imaging camera. The tumor volume and body weight were recorded every two days.

**S12. Hematocylin and eosin (H&E) stained histology.** The MXene QDs (200 μL, 10 mg/kg) were injected separately into the mice via the tail vein. The mice were randomly divided into 3 groups and subjected to variable conditions. This include (i) Control group without any treatment, (ii) MXene QDs being directly *i.v.* injected into the mice, (iii) MXene QDs being directly *i.v.* injected into the mice followed by 808nm laser irradiation for 5 min. Then, the mice were killed at various time points after injection (1, 7, and 14 days, five mice per group at each time point). The major organs (heart, liver, spleen, lung, and kidney) were harvested, fixed in 10% neutral buffered formalin, processed routinely into paraffin, and sectioned at 8 mm for H&E staining.

**S13. Blood routine test (BRT).** The *in vivo* toxicity of MXene QDs was evaluated by BRT experiments. In brief, five healthy Balb/c mice without any treatment were used as the

controls. MXene QDs (200 μL,10 mg/kg) was *i.v.* injected into fifteen healthy Balb/c mice in three groups. After 1, 7, and 14 days of injection, all five mice in a group were sacrificed to collect blood (1 mL) for BRT experiments.

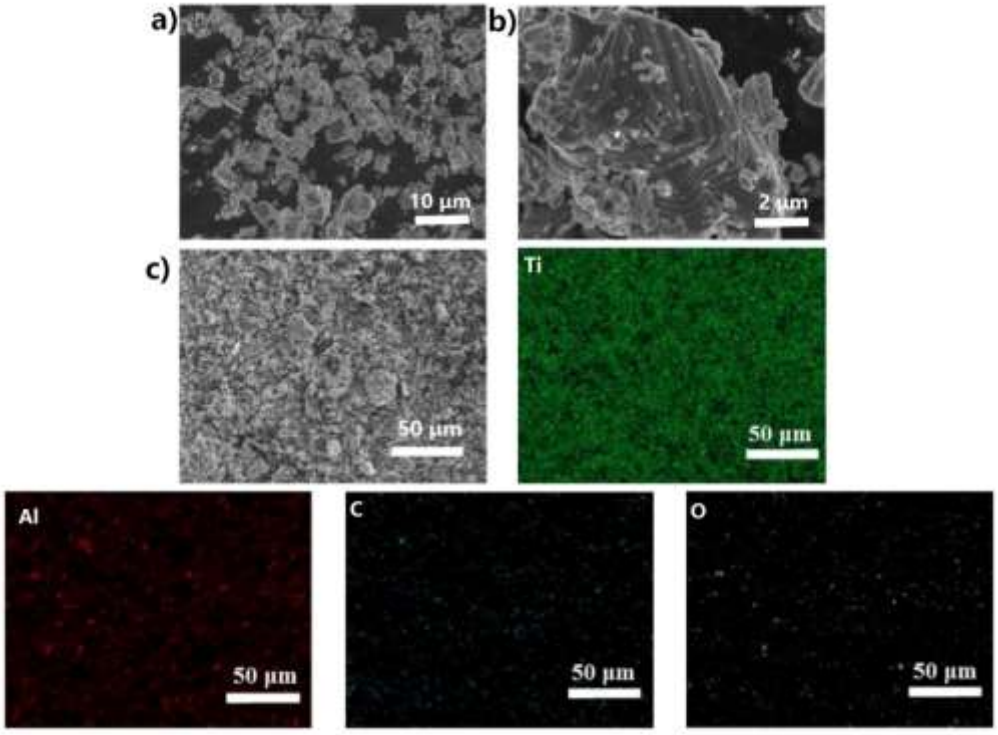


**Fig. S1**. a) Low and b) High magnification SEM images of as-received bulk $Ti_3AlC_2$ powders. c) An SEM image and corresponding elemental analysis of the as-received $Ti_3AlC_2$ powders, showing the presence of Ti, Al, C, and O.

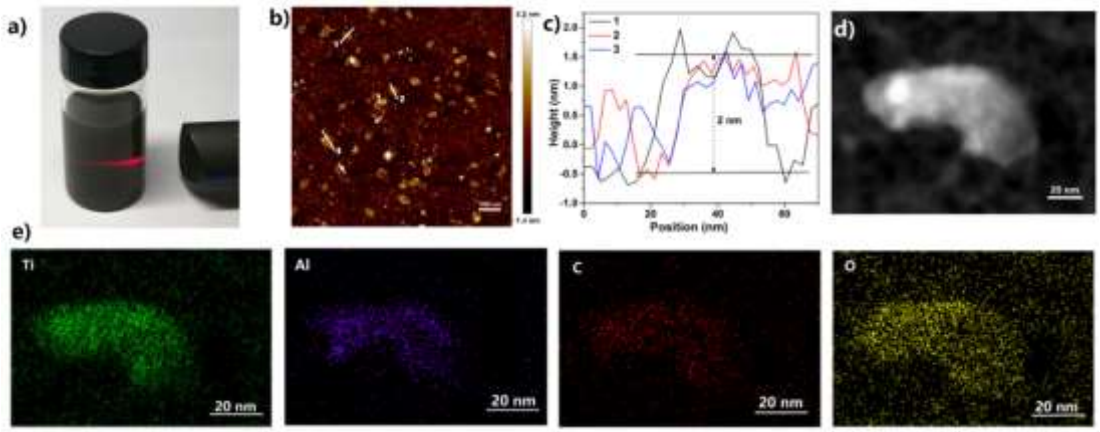

**Fig. S2.** a) Photograph of the MXene nanosheets dispersion in water showing an apparent Tyndall effect. b) An AFM image of MXene nanosheets. c) Height profiles along the white lines in the AFM image, showing an average height of ~2 nm for MXene nanosheets. d) STEM (scale bar = 20 nm). e) EDS mapping (scale bar = 20 nm) of MXene nanosheets.

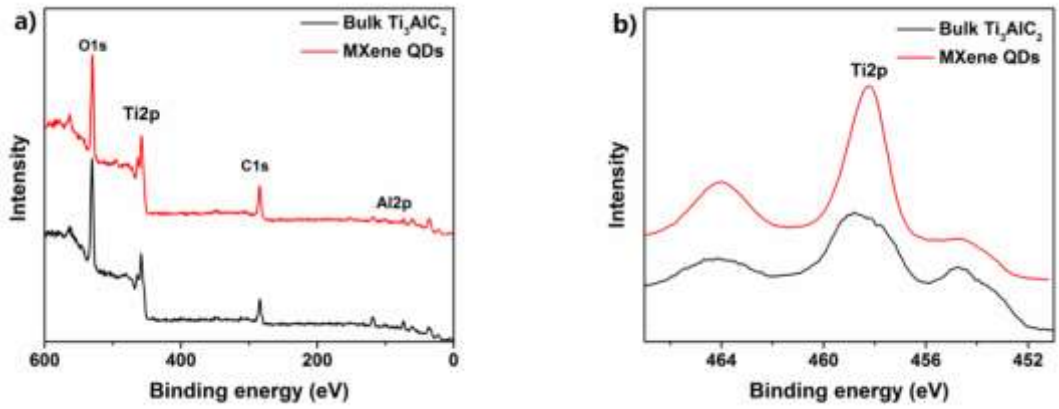


**Fig. S3**. XPS spectra of bulk $Ti_3AlC_2$ powders (black curves) and MXene QDs (Red curves).

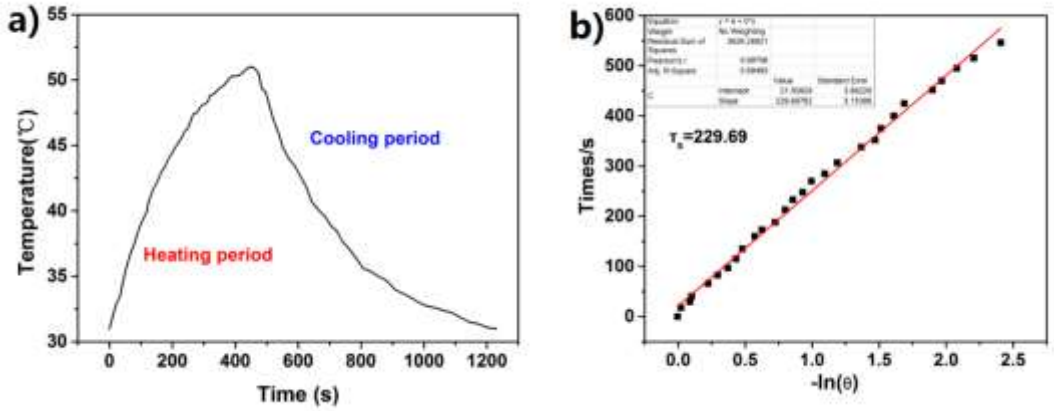


**Fig. S4**. a) Photothermal effect of aqueous dispersion of MXene QDs under irradiation with the NIR laser (808 nm, 1.0 W/cm$^2$), in which the irradiation lasted for 455 s, and then the laser was shut off. b) Time constant for heat transfer from the system is determined to be $\tau_s$= 229.69 s by applying the linear time data from the cooling period (after 455 s) versus negative

natural logarithm of driving force temperature, which is obtained from the cooling period in the panel a.

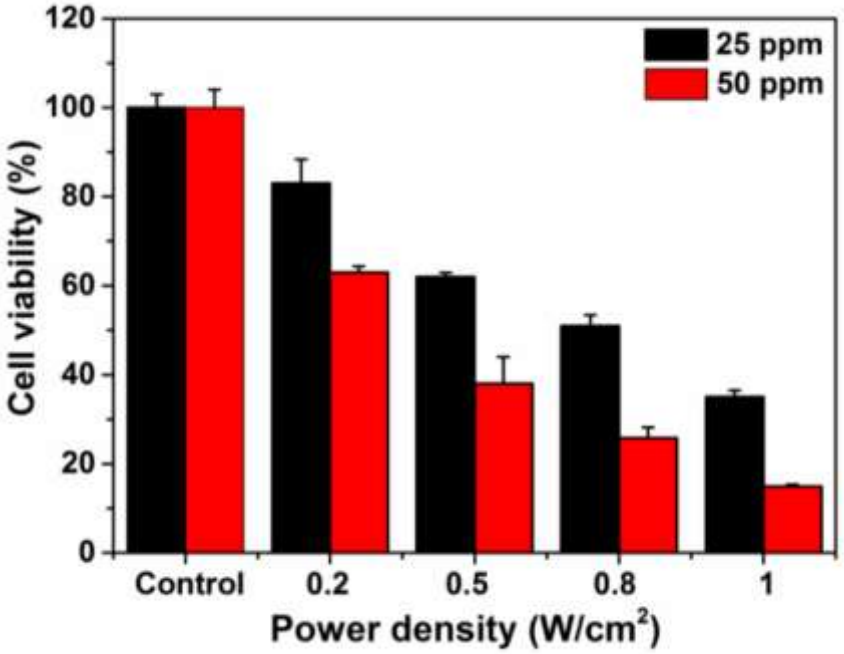


**Fig. S5**. Relative viability of HeLa cells after photothermal ablation induced by MXene QDs at different power densities. The concentrations of MXene QDs was 25 ppm and 50 ppm.

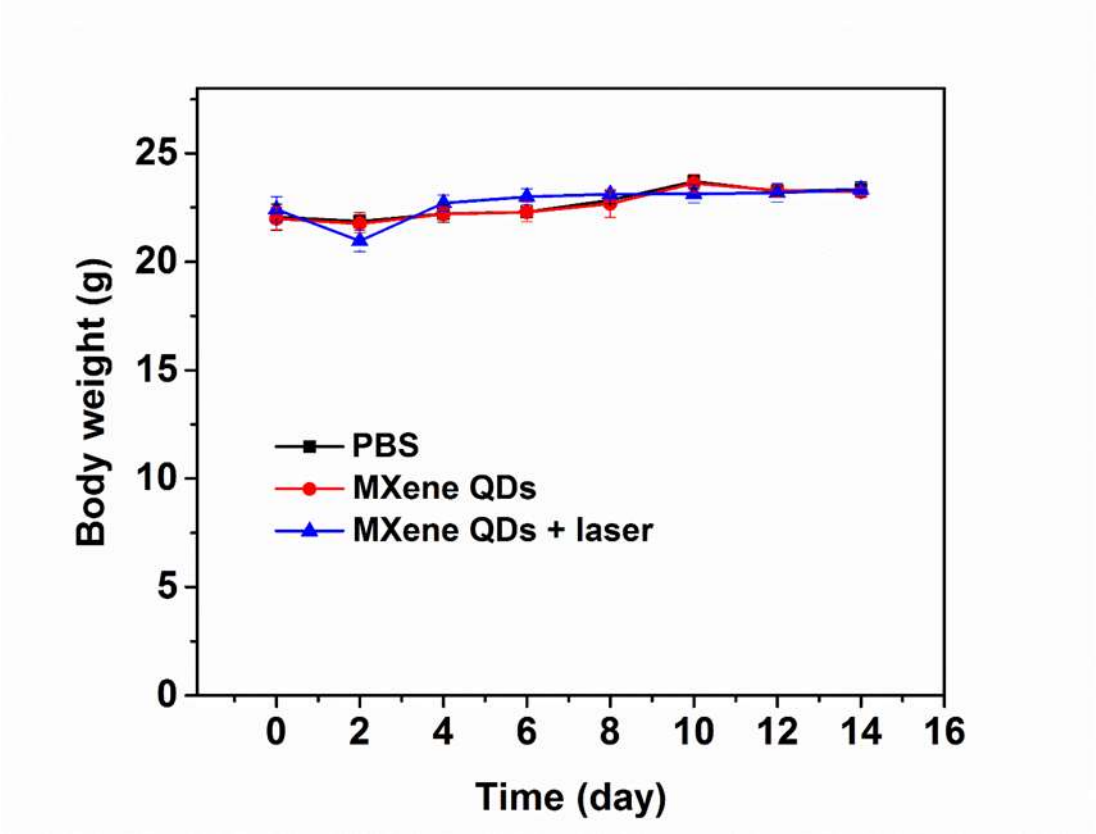


**Fig. S6**. Body weight of nude mice taken at every two days after various treatments with PBS (control), MXene QDs, and MXene QDs followed with 808 nm 0.5 W/cm$^2$ NIR laser irradiation.

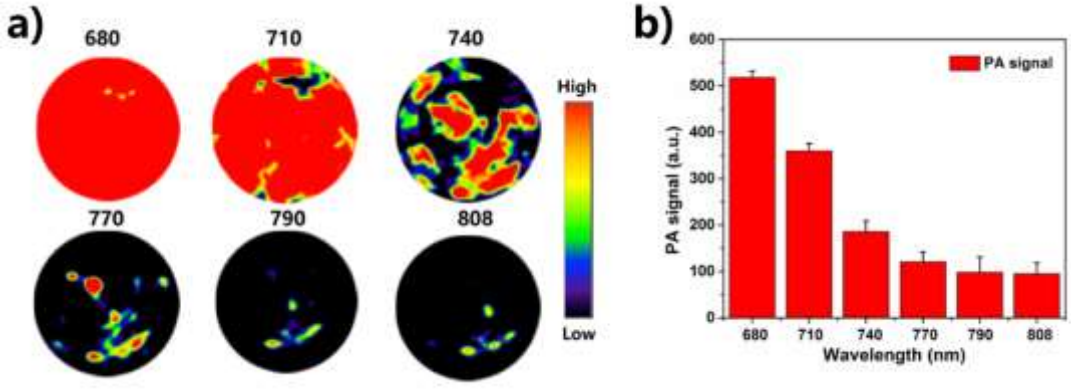


**Fig. S7**. a) PA images of MXene QDs at different excitation wavelengths (680, 710, 740, 770, 790, and 808 nm). b) PA signals and corresponding absorption intensities of MXene QDs at

different excitation wavelengths. The data also suggests that the optimal PA signal occurs at the wavelength of 680 nm which is used in the subsequent PA experiments.

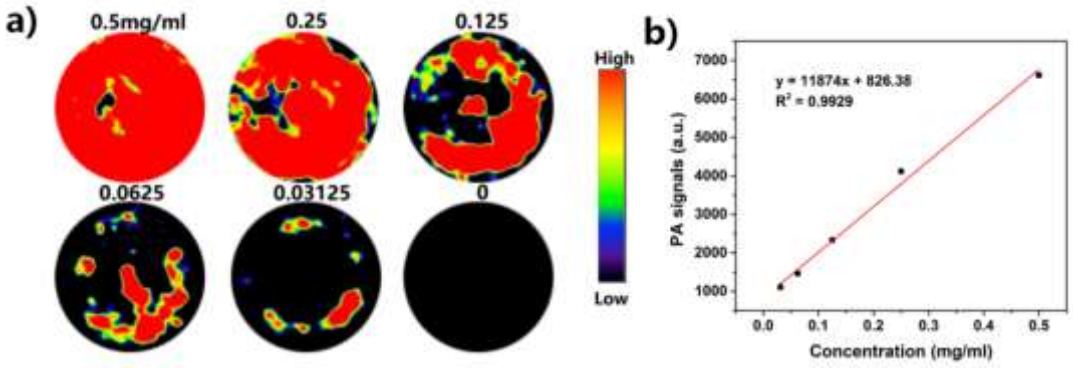


**Fig. S8**. a) PA images of the MXene QDs for different optical densities at 680 nm. b) Corresponding PA signal intensities of the MXene QDs for different concentrations at 680 nm. The PA signal of MXene QDs greatly enhanced with the increase of MXene QDs concentrations and correlated linearly with MXene QDs concentrations, indicating that MXene QDs should be a promising candidate for PA imaging.

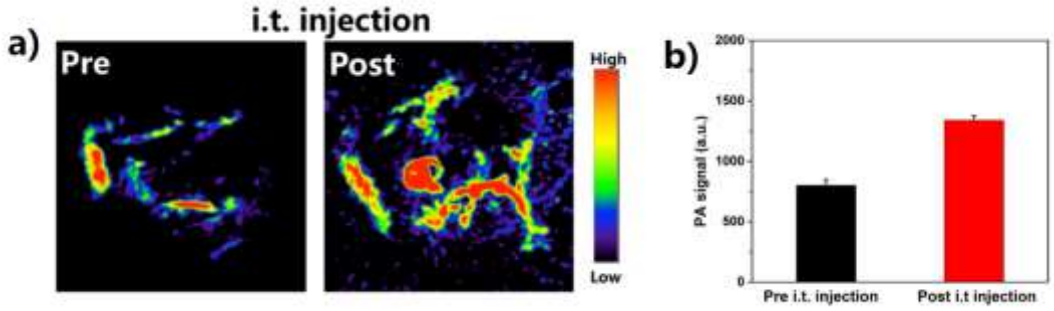


**Fig. S9**. a) PA images and b) PA signal intensities of tumors at 680 nm obtained before and after administration of MXene QDs. Our result indicated the great promise MXene QDs as highly efficient contrast agents for PA imaging guided cancer treatment.

**Table S1.** A comparison of the mass extinction coefficients of several kinds of PPT agents.

| **PPT agents** | **Mass extinction coefficient ($Lg^{-1}cm^{-1}$)** | **Wavelength (nm)** | **References** |
|---|---|---|---|
| Au nanorods | 13.9 | 808 | [2] |
| rGO | 24.6 | 808 | [3] |
| $MoS_2$ | 29.2 | 800 | [4] |
| $WS_2$ | 23.8 | 808 | [5] |
| BP QDs | 14.8 | 808 | [6] |
| $TiS_2$ | 26.8 | 808 | [7] |
| $MoSe_2$ nanodots | 17.4 | 785 | [8] |
| $Bi_2Se_3$ nanosheet | 11.5 | 808 | [9] |

| | | | |
|---|---|---|---|
| TiN NPs | 28.6 | 808 | [10] |
| $Ta_2NiS_5$ | 25.6 | 808 | [11] |
| Graphene oxide(GO) | 3.6 | 808 | [3] |
| $Bi_2Se_3$ nanodots | 3.1 | 808 | [12] |
| $Cu_{2-x}Se$ Nanoparticles | 8.5 | 808 | [13] |
| FeS nanoplates | 15.5 | 808 | [14] |
| $Bi_2S_3$ nanoflowers | 20.5 | 808 | [15] |
| $Ti_3C_2$ nanosheets | 25.2 | 808 | [16] |
| $Ti_xTa_{1-x}S_yO_z$ Nanosheets | 54.1 | 808 | [17] |
| **MXene QDs** | 52.8 | 808 | **This work** |

**Table S2.** A comparison of photothermal conversion efficiency of several kinds of PTT agents.

| **PTT agents** | **Photothermal conversion efficiency** | **Wavelength (nm)** | **References** |
|---|---|---|---|
| $Bi_2Se_3$ nanosheet | 34.6% | 808 | [9] |
| BP QDs | 28.4% | 808 | [6] |
| $Ta_2NiS_5$ | 35% | 808 | [11] |
| $MoSe_2$ nanodots | 46.5% | 785 | [8] |
| $Bi_2Se_3$ nanodots | 50.7% | 808 | [12] |
| $Cu_{2-x}Se$ Nanoparticles | 64.8% | 808 | [13] |
| TiN NPs | 48% | 808 | [10] |

| | | | |
|---|---|---|---|
| $Bi_2S_3$ nanoflowers | 64.3% | 808 | [15] |
| Bismuth sulfide nanorods | 28.1% | 808 | [18] |
| $Ti_3C_2$ nanosheets | 30.6% | 808 | [16] |
| $Ti_xTa_{1-x}S_yO_z$ Nanosheets | 39.2% | 808 | [17] |
| **MXene QDs** | 52.2% | 808 | **This work** |

**Table S3.** Raw data for tumor volumes of HeLa tumors in different groups of nude mice treated with group 1: PBS, group 2: Mxene QDs only, and group 3: Mxene QDs + Laser

| Group 1 | PBS | | | | | |
|---|---|---|---|---|---|---|
| Time | | No.1 | No.2 | No.3 | No.4 | No.5 |
| 0 d | Length (mm) | 7.3 | 7.8 | 7.9 | 7.3 | 8.1 |
| | Width (mm) | 5.9 | 6.1 | 5.8 | 5.7 | 5.2 |
| | Weight (g) | 22.2 | 22.3 | 21.2 | 21.8 | 22.8 |
| | Volume ($mm^3$) | 127.057 | 145.119 | 132.878 | 118.589 | 109.512 |
| 2 d | Length (mm) | 8.4 | 8.8 | 8.9 | 8.6 | 8.3 |
| | Width (mm) | 7.0 | 6.2 | 6.1 | 6.8 | 6.3 |
| | Weight (g) | 22.1 | 22.3 | 21.8 | 21.9 | 21.2 |
| | Volume ($mm^3$) | 205.8 | 169.136 | 168.582 | 198.832 | 164.714 |
| 4 d | Length (mm) | 9.2 | 10.1 | 10.2 | 9.8 | 9.4 |
| | Width (mm) | 7.3 | 7.8 | 6.9 | 6.8 | 7.1 |
| | Weight (g) | 22.9 | 21.8 | 22.0 | 22.1 | 22.3 |
| | Volume ($mm^3$) | 245.134 | 307.242 | 242.811 | 226.579 | 236.927 |
| 6 d | Length (mm) | 9.8 | 10.8 | 10.2 | 10.3 | 11.0 |
| | Width (mm) | 7.8 | 8.2 | 7.9 | 8.5 | 7.8 |
| | Weight (g) | 22.8 | 22.3 | 21.9 | 22.7 | 21.8 |
| | Volume ($mm^3$) | 298.116 | 363.096 | 318.291 | 328.088 | 334.662 |
| 8 d | Length (mm) | 10.9 | 11.2 | 11.5 | 10.7 | 10.8 |

| | | | | | | |
|---|---|---|---|---|---|---|
| | Width (mm) | 9.0 | 8.2 | 8.9 | 10.0 | 8.3 |
| | Weight (g) | 23.0 | 22.8 | 22.7 | 23.0 | 22.7 |
| | Volume ($mm^3$) | 441.45 | 376.544 | 445.458 | 535 | 372.006 |
| 10 d | Length (mm) | 11.2 | 11.8 | 11.3 | 11.9 | 11.2 |
| | Width (mm) | 8.9 | 9.4 | 9.7 | 10.2 | 10.8 |
| | Weight (g) | 23.2 | 23.9 | 24.0 | 23.9 | 23.5 |
| | Volume ($mm^3$) | 443.576 | 521.324 | 531.609 | 619.038 | 653.184 |
| 12 d | Length (mm) | 12.6 | 12.8 | 12.8 | 12.7 | 12.2 |
| | Width (mm) | 11.0 | 10.8 | 11.0 | 10.8 | 10.9 |
| | Weight (g) | 23.5 | 23.0 | 23.2 | 23.5 | 23.1 |
| | Volume ($mm^3$) | 762.3 | 746.496 | 774.4 | 740.664 | 724.741 |
| 14 d | Length (mm) | 13.2 | 13.8 | 12.9 | 13.8 | 13.7 |
| | Width (mm) | 12.1 | 11.9 | 12.8 | 12.1 | 12.0 |
| | Weight (g) | 23.5 | 23.8 | 22.9 | 23.1 | 23.4 |
| | Volume ($mm^3$) | 996.306 | 977.109 | 1056.77 | 1010.23 | 986.4 |

| Group 2 | MXene QDs | | | | | |
|---|---|---|---|---|---|---|
| Time | | No.1 | No.2 | No.3 | No.4 | No.5 |
| 0 d | Length (mm) | 7.2 | 7.4 | 7.0 | 7.1 | 7.8 |
| | Width (mm) | 6.2 | 6.1 | 5.9 | 5.9 | 5.8 |
| | Weight (g) | 22.1 | 22.1 | 21.2 | 21.8 | 22.7 |
| | Volume ($mm^3$) | 138.384 | 137.677 | 121.135 | 123.576 | 131.196 |
| 2 d | Length (mm) | 8.1 | 8.5 | 8.6 | 8.1 | 8.9 |
| | Width (mm) | 7.2 | 6.3 | 6.1 | 6.6 | 6.9 |
| | Weight (g) | 22.3 | 22.1 | 21.6 | 21.5 | 21.3 |
| | Volume ($mm^3$) | 209.952 | 168.683 | 160.003 | 176.418 | 211.865 |
| 4 d | Length (mm) | 8.6 | 10.2 | 10.0 | 9.5 | 9.4 |
| | Width (mm) | 7.6 | 7.2 | 7.6 | 6.3 | 7.5 |
| | Weight (g) | 22.0 | 21.9 | 22.6 | 22.5 | 22.0 |
| | Volume ($mm^3$) | 248.368 | 264.364 | 288.8 | 188.528 | 264.375 |
| 6 d | Length (mm) | 9.9 | 10.0 | 10.7 | 10.6 | 10.8 |
| | Width (mm) | 7.9 | 9.0 | 7.5 | 8.6 | 7.3 |
| | Weight (g) | 22.8 | 22.3 | 21.9 | 22.7 | 21.8 |
| | Volume ($mm^3$) | 308.93 | 405 | 300.938 | 391.988 | 287.766 |
| 8 d | Length (mm) | 10.1 | 11.3 | 11.2 | 10.3 | 11.2 |
| | Width (mm) | 9.3 | 9.0 | 9.0 | 10.1 | 8.1 |
| | Weight (g) | 23.1 | 23.0 | 23.3 | 22.1 | 21.9 |

| | | | | | | |
|---|---|---|---|---|---|---|
| | Volume ($mm^3$) | 436.755 | 457.65 | 453.6 | 525.352 | 367.416 |
| 10 d | Length (mm) | 11.0 | 11.9 | 11.6 | 11.9 | 11.3 |
| | Width (mm) | 8.8 | 9.6 | 9.2 | 10.3 | 10.4 |
| | Weight (g) | 23.1 | 23.8 | 24.2 | 23.4 | 23.6 |
| | Volume ($mm^3$) | 425.92 | 548.352 | 490.913 | 631.236 | 611.104 |
| 12 d | Length (mm) | 12.5 | 12.9 | 12.4 | 12.3 | 12.2 |
| | Width (mm) | 11.2 | 11.3 | 11.3 | 10.9 | 10.8 |
| | Weight (g) | 22.9 | 23.1 | 23.3 | 23.6 | 23.5 |
| | Volume ($mm^3$) | 784 | 823.601 | 791.618 | 730.682 | 711.504 |
| 14 d | Length (mm) | 13.3 | 13.9 | 12.5 | 12.5 | 13.6 |
| | Width (mm) | 12.6 | 11.8 | 12.6 | 12.4 | 12.5 |
| | Weight (g) | 23.2 | 23.3 | 23.4 | 22.9 | 23.3 |
| | Volume ($mm^3$) | 1055.75 | 967.718 | 992.25 | 961 | 1062.8 |

| Group 3 | MXene QDs + Laser | | | | | |
|---|---|---|---|---|---|---|
| Time | | No.1 | No.2 | No.3 | No.4 | No.5 |
| 0 d | Length (mm) | 6.9 | 7.2 | 6.9 | 7.8 | 7.5 |
| | Width (mm) | 5.5 | 5.1 | 6.2 | 6.1 | 6.1 |
| | Weight (g) | 22.3 | 23.1 | 22.8 | 21.6 | 22.3 |
| | Volume ($mm^3$) | 104.363 | 93.636 | 132.618 | 145.119 | 139.538 |
| 2 d | Length (mm) | 0 | 0 | 0 | 0 | 0 |
| | Width (mm) | 0 | 0 | 0 | 0 | 0 |
| | Weight (g) | 21.2 | 21.2 | 20.3 | 20.6 | 21.5 |
| | Volume ($mm^3$) | 0 | 0 | 0 | 0 | 0 |
| 4 d | Length (mm) | 0 | 0 | 0 | 0 | 0 |
| | Width (mm) | 0 | 0 | 0 | 0 | 0 |
| | Weight (g) | 22.4 | 23.1 | 22.5 | 22.4 | 23.1 |
| | Volume ($mm^3$) | 0 | 0 | 0 | 0 | 0 |
| 6 d | Length (mm) | 0 | 0 | 0 | 0 | 0 |
| | Width (mm) | 0 | 0 | 0 | 0 | 0 |
| | Weight (g) | 22.5 | 23.3 | 22.9 | 23.4 | 22.9 |
| | Volume ($mm^3$) | 0 | 0 | 0 | 0 | 0 |
| 8 d | Length (mm) | 0 | 0 | 0 | 0 | 0 |
| | Width (mm) | 0 | 0 | 0 | 0 | 0 |

| | | | | | | |
|---|---|---|---|---|---|---|
| | Weight (g) | 23.1 | 23.2 | 22.9 | 23.2 | 23.2 |
| | Volume ($mm^3$) | 0 | 0 | 0 | 0 | 0 |
| 10 d | Length (mm) | 0 | 0 | 0 | 0 | 0 |
| | Width (mm) | 0 | 0 | 0 | 0 | 0 |
| | Weight (g) | 23.1 | 22.5 | 23.6 | 23.4 | 23.1 |
| | Volume ($mm^3$) | 0 | 0 | 0 | 0 | 0 |
| 12 d | Length (mm) | 0 | 0 | 0 | 0 | 0 |
| | Width (mm) | 0 | 0 | 0 | 0 | 0 |
| | Weight (g) | 23.1 | 23.2 | 22.5 | 23.6 | 23.5 |
| | Volume ($mm^3$) | 0 | 0 | 0 | 0 | 0 |
| 14 d | Length (mm) | 0 | 0 | 0 | 0 | 0 |
| | Width (mm) | 0 | 0 | 0 | 0 | 0 |
| | Weight (g) | 22.8 | 23.7 | 23.6 | 23.4 | 23.2 |
| | Volume ($mm^3$) | 0 | 0 | 0 | 0 | 0 |

## References


1. D. K. Roper, W. Ahn and M. Hoepfner, *J Phys Chem C Nanomater Interfaces*, 2007, **111**, 3636-3641.
2. J. T. Robinson, K. Welsher, S. M. Tabakman, S. P. Sherlock, H. Wang, R. Luong and H. Dai, *Nano Res*, 2010, **3**, 779-793.
3. J. T. Robinson, S. M. Tabakman, Y. Liang, H. Wang, H. S. Casalongue, D. Vinh and H. Dai, *J Am Chem Soc*, 2011, **133**, 6825-6831.
4. S. S. Chou, B. Kaehr, J. Kim, B. M. Foley, M. De, P. E. Hopkins, J. Huang, C. J. Brinker and V. P. Dravid, *Angew Chem Int Ed Engl*, 2013, **52**, 4160-4164.
5. L. Cheng, J. Liu, X. Gu, H. Gong, X. Shi, T. Liu, C. Wang, X. Wang, G. Liu, H. Xing, W. Bu, B. Sun and Z. Liu, *Adv Mater*, 2014, **26**, 1886-1893.
6. Z. Sun, H. Xie, S. Tang, X. F. Yu, Z. Guo, J. Shao, H. Zhang, H. Huang, H. Wang and P. K. Chu, *Angew Chem Int Ed Engl*, 2015, **54**, 11526-11530.
7. X. X. Qian, S. D. Shen, T. Liu, L. Cheng and Z. Liu, *Nanoscale*, 2015, **7**, 6380-6387.
8. L. Yuwen, J. Zhou, Y. Zhang, Q. Zhang, J. Shan, Z. Luo, L. Weng, Z. Teng and L. Wang, *Nanoscale*, 2016, **8**, 2720-2726.
9. H. Xie, Z. Li, Z. Sun, J. Shao, X. F. Yu, Z. Guo, J. Wang, Q. Xiao, H. Wang, Q. Q. Wang, H. Zhang and P. K. Chu, *Small*, 2016, **12**, 4136-4145.
10. W. He, K. Ai, C. Jiang, Y. Li, X. Song and L. Lu, *Biomaterials*, 2017, **132**, 37-47.
11. H. Zhu, Z. Lai, Y. Fang, X. Zhen, C. Tan, X. Qi, D. Ding, P. Chen, H. Zhang and K. Pu, *Small*, 2017, **13**.
12. F. Mao, L. Wen, C. Sun, S. Zhang, G. Wang, J. Zeng, Y. Wang, J. Ma, M. Gao and Z. Li, *ACS Nano*, 2016, **10**, 11145-11155.

13. S. Zhang, C. Sun, J. Zeng, Q. Sun, G. Wang, Y. Wang, Y. Wu, S. Dou, M. Gao and Z. Li, *Adv Mater*, 2016, **28**, 8927-8936.
14. K. Yang, G. B. Yang, L. Chen, L. Cheng, L. Wang, C. C. Ge and Z. Liu, *Biomaterials*, 2015, **38**, 1-9.
15. Z. Y. Xiao, C. T. Xu, X. H. Jiang, W. L. Zhang, Y. X. Peng, R. J. Zou, X. J. Huang, Q. Liu, Z. Y. Qin and J. Q. Hu, *Nano Research*, 2016, **9**, 1934-1947.
16. H. Lin, X. G. Wang, L. D. Yu, Y. Chen and J. L. Shi, *Nano Lett*, 2017, **17**, 384-391.
17. H. Zhang, C. Tan, L. Zhao, P. Yu, Y. Huang, B. Chen, Z. Lai, X. Qi, M. H. Goh, X. Zhang, S. Han, X. J. Wu, Z. Liu and Y. Zhao, *Angew Chem Int Ed Engl*, 2017, DOI: 10.1002/anie.201703597.
18. J. Liu, X. Zheng, L. Yan, L. Zhou, G. Tian, W. Yin, L. Wang, Y. Liu, Z. Hu, Z. Gu, C. Chen and Y. Zhao, *ACS Nano*, 2015, **9**, 696-707.